A Hybrid Fuel Cell/Battery Wheelchair — Modeling, Simulation and Experimentation

David Bouquain, Benjamin Blunier and Abdellatif Miraoui
Transport and Systems Laboratory (SeT) – EA 3317/UTBM
University of Technology of Belfort-Montbéliard, France
Email: (david.bouquain,benjamin.blunier,abdellatif.miraoui)@utbm.fr

***Abstract*—This paper presents a hybrid fuel cell/battery wheelchair modeling and design. In this system, the fuel cell acts as a range extender allowing this component to have a low dynamic. The peaks of power are given by a battery. The control of the fuel cell system and the control of the overall system is presented together with an experimental validation.**

***Index Terms*—Hybridization, Fuel cell, battery, modeling, experimentation**

I. Introduction

New technologies of motorization, clean energy sources and wireless communication can be also used to improve the mobility and independence of handicapped peoples. The aim of the project is to use new software and energy technologies on a wheelchair: assistance during displacements, geographic location, remote communication with other systems, monitoring of the state of health thanks to appropriate biometric sensors linked to the system. A prototype using many of these technologies, illustrated on Fig. 1 is under developments.

Figure 1. Wheelchair under developments

This paper introduces the design and tests of a hybrid solution for an intelligent electrical wheelchair. It is based on a structure using a 300 watts fuel cell stack connected to a lead-acid battery thanks to a DC/DC buck converter. The lead battery is not nowadays the battery the most adapted for the electric vehicle: this kind of accumulator is heavy and has a low energy density compared to Li-Ion accumulator for example [1]. However it can handle peaks of current very well and it is still the less expensive technology. Fuel cells are not reversible and have big time transients which are not fully compatible with electrical traction, that is why fuel cells are always associated with a reversible power or energy source (supercapacitors or battery) which can handle peaks of power, but also, recover energy during braking phases.

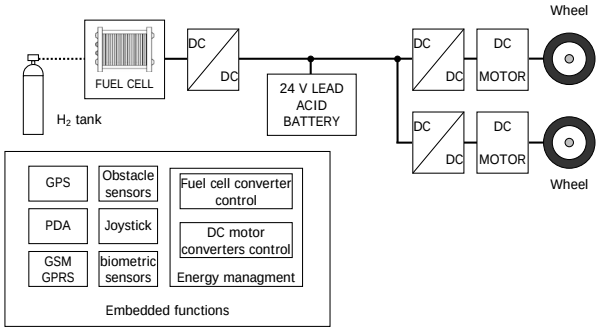

Figure 2. Overall wheelchair system overview

For a first approach, a rather simple but robust structure was chosen to validate the relevance of using a fuel cell system in such a system. The aim is to have the most simple and less expensive system which does not need any expensive components and big computation power. In a second step, structures similar to the ones introduced by the authors of [2] will be investigated. Wang [3], [4] propose a low-cost quasi-resonant dc-dc converter for fuel cell that could also be used to improve the system efficiency compared to a simple buck converter keeping the costs relatively low.

In the actual structure, the batteries provide the peaks of power and the fuel cell is sized to provide nearly the average power. Moreover the battery can also be used during the phase of regenerative braking (not investigated in this paper).

The paper is organized as follows: in a first part, an overview of the architecture and the components of the wheelchair is given. The intelligent part of the system will be shortly introduced. The second part presents the modeling of the system and its control. The last part presents the simulation and experimentation results.

II. System Overview

The figure 2 gives an overview of the wheelchair system. The fuel cell used in this application is a Polymer Electrolyte

Fuel Cell (PEFC). It works at low temperature and at atmospheric pressure on the cathode side. Its maximum power is about 300 watts and the voltage is between 30 and 58 volts. A DC/DC buck converter between the stack and the dc link allows the fuel cell current to be controlled. Two lead-acid batteries in series impose the DC bus voltage to be around 24 volts depending on the state of charge of the battery. The power converters for the DC motors are fully bidirectional (voltage and current) allowing regenerative braking. The signal conditioning and processing and the control are done with a micro-autobox from dSPACE embedded into the wheelchair. This system allows rapid prototyping and implementation in a embedded real time system the control laws developed under Matlab-Simulink.

Other functionalities, out of the scope of the paper, are also implemented in the wheelchair : geographic location by GPS, remote control thanks to a personal digital assistant (PDA), mobile telephony by using GSM network, obstacles detection, joystick for on-board control and biometric sensors.

III. System Modelling and Control

A complete model of the electrical part of the system has been built to size the storage components (hydrogen tank and batteries) according a driving profile. This model permits also to test virtually the control laws and energy management strategies before their implementation on the real system.

This section presents the models of the wheelchair, the fuel cell stack and the batteries.

A. Wheelchair Model

The model of the wheelchair as for every vehicles models is based on the mechanical forces acting on the vehicle. The electrical power calculation of the wheelchair (P_e) takes into account the dynamics of the vehicle ($\mathrm{d}v/\mathrm{d}t$), the speed v, the road grade (α), its total mass (M_v), the aerodynamic drag coefficient (C_x), the wheelchair front surface including the driver (S), the rolling coefficient (C_r), the drive train efficiency (η_d) [5].

$$P_{\mathrm{e}} = \frac{v}{\eta_d}\left(M_{\mathrm{v}}\frac{\mathrm{d}v}{\mathrm{d}t} + \frac{1}{2}\rho_{\mathrm{air}}\,v^2\,S\,C_{\mathrm{x}} + M_{\mathrm{v}}\,g\,\sin\alpha + M_{\mathrm{v}}\,g\,C_{\mathrm{r}}\,\cos\alpha\right) \quad (1)$$

For a given driving cycle (speed and road grade profiles), the wheelchair power can be computed from (1). The total nominal power of the wheelchair simulated and measured is arround 400 watts.

B. Fuel cell model

As the power required is low, the fuel cell works at atmospheric pressure. The air is supplied with three fans at a high stoechiometric ratio. The cooling of the fuel cell is done with the same fans than the air supply.

The high stoechiometric ratio ensure that there is nearly no oxygen depletion and no electrodes flooding. As the fuel cell system acts as a range extender (its power is lower than the nominal power) the dynamic does not need to be high. For this reason, but also to increase the lifetime of the fuel cell, the control maintains the dynamic of the fuel cell very low (see sec. III-D).

Considering this remarks, it can be assumed that the fuel cell is almost always in steady state : in this case a static model of the fuel cell can be used. For higher powers, the static characteristic cannot be used to describe the fuel cell system : the compressor and the air dynamic (air pressure inside the channels), as well as the water content of the membrane which affects the membrane resistance have to be considered. The authors presented such a model in [6].

The static characteristic is therefore described as a current (I)-voltage (V) function [7]:

$$V_{\mathrm{stack}}(I) = E_0 - R\,I_{\mathrm{stack}} - A\,\ln(I_{\mathrm{stack}}) + m\,\exp(n\,I_{\mathrm{stack}}) \quad (2)$$

where E_0, R, A, m and n are empirical coefficients to be determined for the investigated fuel cell stack.

C. Battery model

The purpose of the battery simulations is to be able to predict the performance of the wheelchair, in terms of range, acceleration, speed, etc. For this system, the speed of the vehicle changes fairly slowly, and the dynamic behaviour of the battery is not significant. Therefore, in this paper, only the basic equivalent circuit of a battery (capacitance with a serie resistance) is used.

1) Open circuit voltage: The batteries used in the system are lead-acid batteries: the open circuit voltage E is approximatively proportional to the state of charge of the battery [8]. Considering the variable DoD, representing the depth of discharge equal to zero when the battery is fully charged and one when empty, then the simple formula (only valid for lead-acid batteries) for the open circuit voltage is [8]:

$$E = n\,(2.15 - DoD \cdot (2.15 - 2.00)) \quad (3)$$

where n is the number of cells in the battery.

2) Capacity: The capacity of a battery is reduced if the current is drawn more quickly: drawing 1 amperes for 10 hours does not take the same charge from a battery as running 10 amperes for 1 hour.

This phenomenon has to be taken into account for such an application to be able to predict autonomy of the wheelchair. Moreover, it is important to be able to predict the effect of current on capacity for the design process but also to measure the charge left in the battery.

For this application, the Peukert model the battery behavior is used [8]. This model is not very accurate at low currents but for high currents it models the battery behaviour well enough.

The Peukert capacity (C_p) is calculated as follows :

$$C_p = I^k\,T \quad (4)$$

where k is constant called the Peukert coefficient (arround 1.2 for lead-acid batteries). The Peukert capacity is equivalent

to the normal ampere-hours capacity for a battery discharges at 1 A.

If the capacity is given, for example, for $T = 10$ hours, the Peukert capacity will be calculated as follows :

$$C_p = \underbrace{\left(\frac{C_{10}}{10}\right)^k}_{I} \cdot 10 \tag{5}$$

If a current I flows from the battery, then, from the point of view of the battery capacity, the current that appear to flow out of the battery is I^k. Therefore, the capacity which is removed from the battery is:

$$C_R\ [\text{Ah}] = \int \frac{I^k}{3\,600}\,\mathrm{d}t \tag{6}$$

The initial condition of C_R have to be given for the simulation :

$$C_{R,\text{init}} = C_p \cdot DoD_{\text{init}} \tag{7}$$

where DoD_{init} is the initial depth of discharge.

3) Depth of Discharge: The depth of discharge of the battery is the ratio of the charge removed to the original capacity:

$$DoD = \frac{C_R}{C_p} \tag{8}$$

The calcultated value of DoD is used to compute the open circuit voltage given by (3).

D. Control strategy

1) Fuel Cell System Control: The fuel cell system has to be controlled properly with a simple, robust and cheap control. The control strategy is summarized in Fig. 3:

- the oxygen has to be supplied at a rate proportional to the current : in this case, the voltage of the fans (0–12 volts) is controlled with the DC/DC converter duty-cycle α_{fans} proportionally to the fuel cell current. The rotational speed of the fans is almost proportional to their voltage. As the stoechiometric ratio is maintained high, a change of speed will not affect to much the voltage. Tests shown that the speed could be maintained at the same value over a wide current range without affecting the voltage (this is only valid for atmospheric and low power fuel cells) ;
- the hydrogen has to be supplied at a rate proportional to the current : this is achieved by a valve without any regulation ;
- the temperature has to be maintained lower than the maximum value (T_{max}) which is arround 50 °C for the investigated fuel cell. However a higher temperature will give a higher voltage: it is then better to maintain the temperature as high as possible but always below the maximum temperature. When the fuel cell temperature approach a given limit temperature ($T_{\text{max}} - \Delta T$) of the fuel cell, a speed reference (duty-cycle α_{temp}), proportional to the stack temperature, is added to the speed reference of the fans α_{fans};
- when the water and nitrogen accumulate at the anode side, the fuel cell stack voltage drops below its normal voltage (given by the polarization curve). In this case, the anode has to be purged to remove these products. Practically, at given current, the actual fuel cell voltage is compared to the polarization curve: if the actual voltage is too low (*e.g.*, 10 % below the polarization curve), the anode is purged during 1 s.

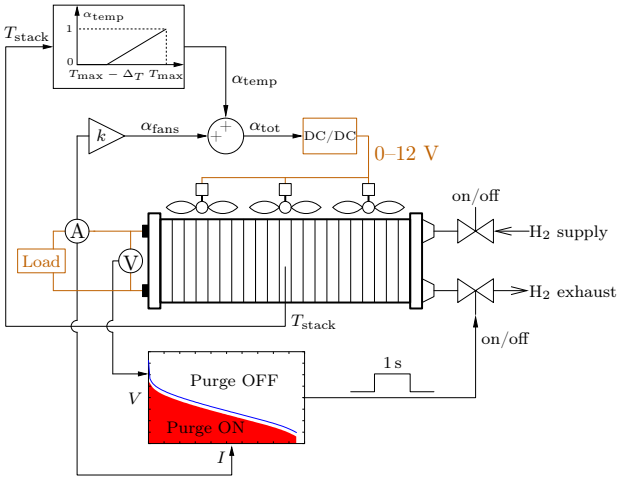

Figure 3. Fuel cell control strategy

2) Overall System Control: The overall system control has to give a current reference to the fuel cell. The dynamic of the fuel cell can be low as it acts as a range extender. When sudden changes occur in the load power, the fuel cell still works at its previous working point and the battery provides the difference. The fuel cell will take time to reach the desired power: until that time, the battery supplies the load (in the case of a positive current step) or is charged by the fuel cell (in the case of a negative current step).

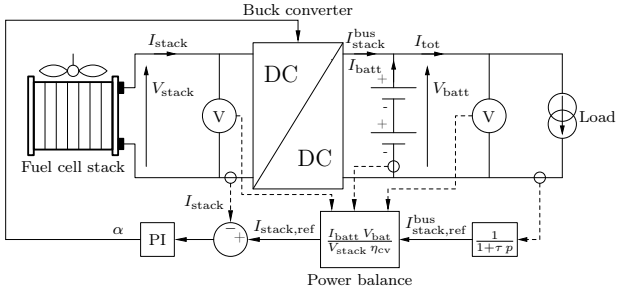

Figure 4. Overall system control strategy

The time with which the fuel cell takes to reach the desired power depends on the control strategy. In this case, the load current (I_{load}) is filtered through a first-order transfer function as shown in Fig. 4: the output of this function is the fuel cell stack current reference on the DC bus ($I^{\text{bus}}_{\text{stack}}$) which gives the stack current reference I_{stack} thanks to the DC/DC converter power balance: $V_{\text{stack}}\,I_{\text{stack}}\,\eta_{\text{cv}} = V_{\text{batt}}\,I^{\text{bus}}_{\text{stack}}$, where η_{cv} is the converter efficiency. This current I_{stack} reference is obviously

limited to the maximum current the fuel cell can supply. Over this current, the battery has to supply the remaining current.

IV. Simulation and Experimental Results

A. Fuel cell tests and parameters identification

Tests have been performed on the fuel cell to identify the empirical parameters given in (2). These parameters have been identified thanks to a non-linear regression (Levenberg-Marquardt) and the results are shown in Fig. 5.

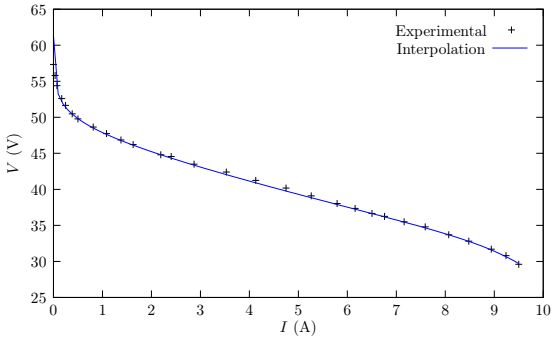

(a) Fuel cell stack $V - I$ characteristic

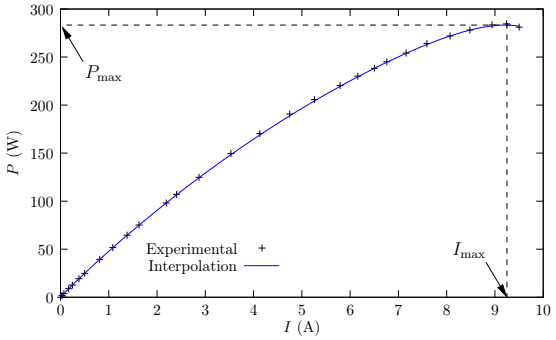

(b) Fuel cell stack $P - I$ characteristic

Figure 5. Fuel cell polarization curves

Dynamic tests in Fig. 6 show that the polarization curve can be used to estimate in real-time, with a good accuracy, the stack voltage from the current measurement. This estimation is needed to detect any voltage drop due to nitrogen accumulation in the anode channels. If a better accuracy is needed, the polarization curve could take into account temperature effects as it has been described in [5], [9].

B. Battery tests and parameters identification

To validate and identify the battery parameters, the same current profile is imposed to the real battery and the battery model. The measured and predicted voltage are compared for a set of parameters and the integral of the quadratic error is computed. The optimal set of parameters is the one which give the smallest error and has been found by mean of a Simplex optimisation algorithm. The results are given for the simulated (with the optimal set of parameters) and experimental powers on Fig. 7. These parameters permit the instantaneous voltage (serie resistance effects) as well as the DoD to be computed.

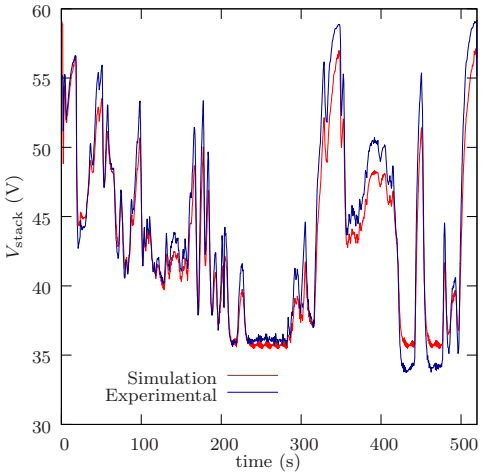

Figure 6. Simulated and experimental stack voltage over a current profile

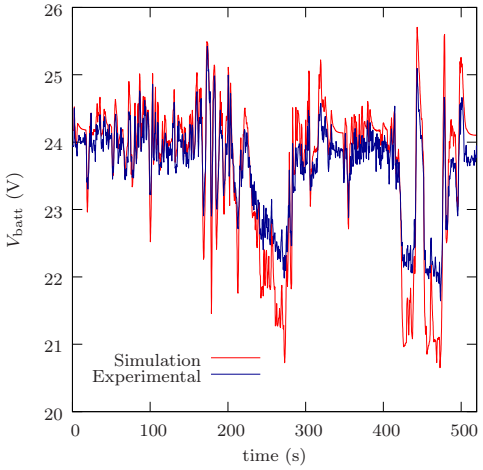

Figure 7. Simulated and experimental battery voltage over a current profile

C. Overall system tests

Tests have been performed on the test bench shown in Fig. 8. This system can be directly integrated in the wheelchair if the hydrogen storage is provided. In this case, a metal hydride tank with a capacity of 25 g (275 StdL) at 20 bar will be used.

The current load profile, computed from the electrical power measurement of a real wheelchair during a 520 s driving mission, is imposed by means of an active load. Several tests have been performed for the same load current profile and for 4 filter time constants τ (see Fig. 9). By adjusting τ, the fuel cell stack current dynamic can be controlled: he higher it is, the lower is the dynamics.

DC currents for $\tau = 2$ s are shown in Fig. 10. It can be seen on the one hand that the stack current is smooth and on the other hand that the battery delivers or recovers the current during transients but also when the stack power is not sufficient (arround 250 s).

The temperature management works also relatively well as T_{stack} is maintained as high as possible but always below the maximum temperature T_{max}: when the temperature is higher

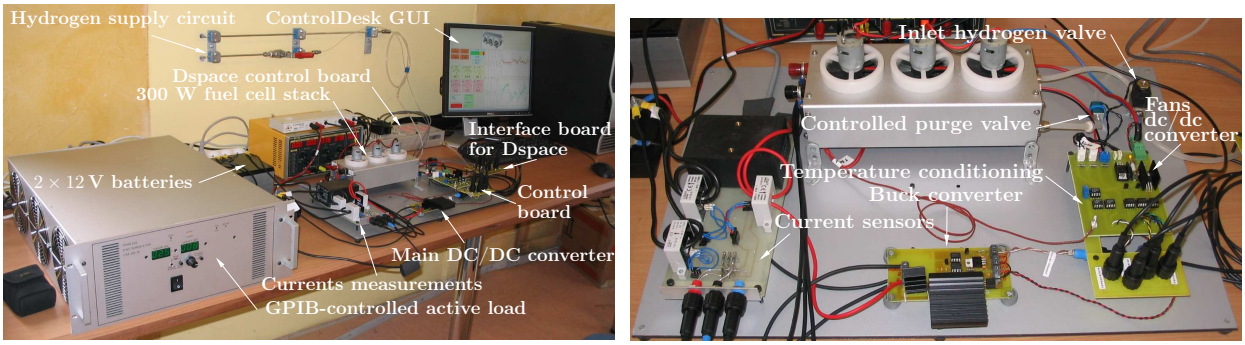

(a) Overall system test bench

(b) Fuel cell system

Figure 8. Fuel cell system tests bench

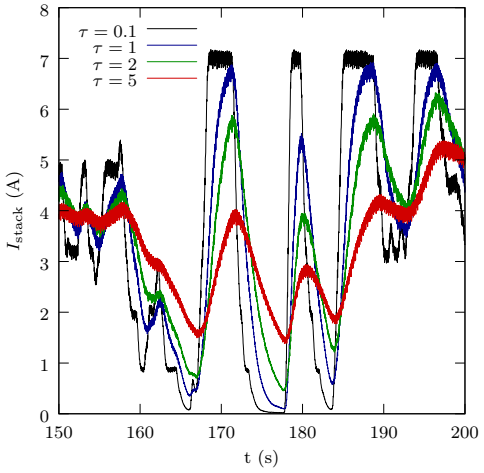

(a) Fuel cell stack current

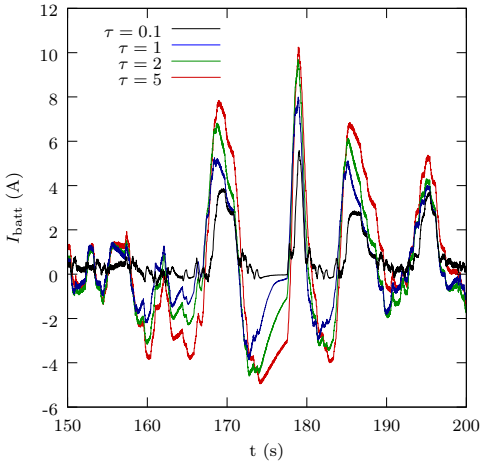

(b) Batteries current

Figure 9. Stack and batteries currents for several values of τ

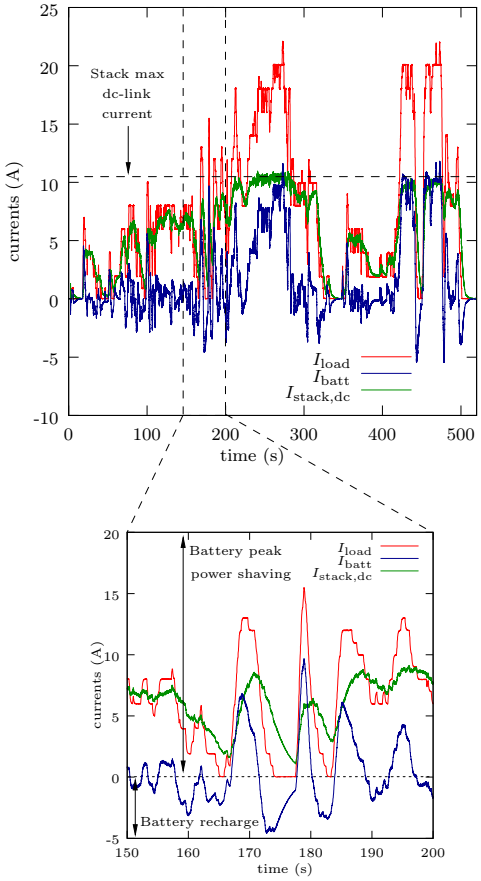

Figure 10. DC-link currents for $\tau = 2\,\mathrm{s}$

than $T_{\max} - \Delta T$, the fans speed is increased proportionally to T_{stack} to maintain the temperature below $T_{\max}$. When colling is not needed (*i.e.*, when $T_{\text{stack}} < T_{\max} - \Delta T$), the fans speed only depends on the stack current.

The stack voltage estimation permits the purge to be enabled. The figure 12 shows that when the actual stack voltage drops below 90 % of the predicted voltage (arround 421 s), the purge is enabled during 1 s. The purge helps the voltage to recover at a normal value at about 422 s.

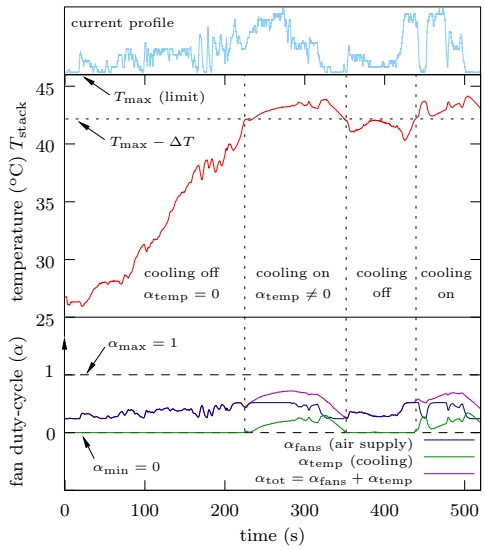

Figure 11. Temperature management

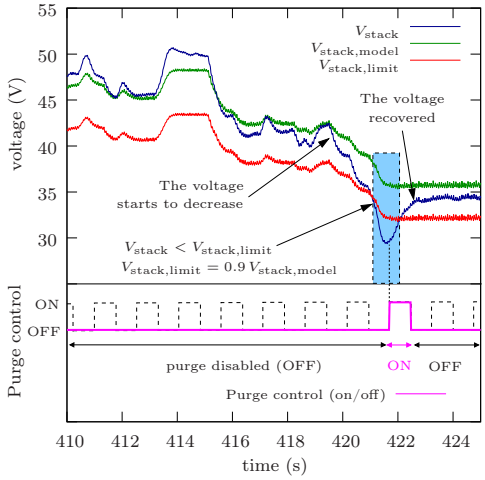

Figure 12. Purge control

V. Conclusion

A hybrid fuel cell/battery wheelchair has been modeled and designed. The fuel cell in this system acts as a range extender allowing this component to have a low dynamic. The control of the fuel cell system and the control of the overall system has been presented and validated experimentaly on the system. Tests have shown that a very simple and cheap control strategy which does not require any high computation power can give very good results: temperature management, purges, energy management.

This system shows the advantages of hybridization of a fuel cell with batteries: the fuel cell system, which is the most expensive component, can be downsized as it does not have to supply the maximum power. When the vehicle is at its full power, both the batteries and the fuel cell system supply power.

However, the advantages in terms of compacity are not so obvious when using a atmospheric fuel cell (see Fig. 13). Measurements of the size of the fuel cell system have shown that its specific energy is about 80 Wh/kg which is two times the one of lead-acid batteries but the energy densities are nearly the same: 103 Wh/L for the fuel cell system and 100 Wh for the lead-acid batteries. Comparing the fuel cell system to Li-ion batterie are worse as these batteries offer 100–200 Wh/kg and 200–400 Wh/L. Moreover, grid-to-wheel efficiency of batteries is at least three times more higher than the one of fuel cells when the hydrogen is produced from electrolysis.

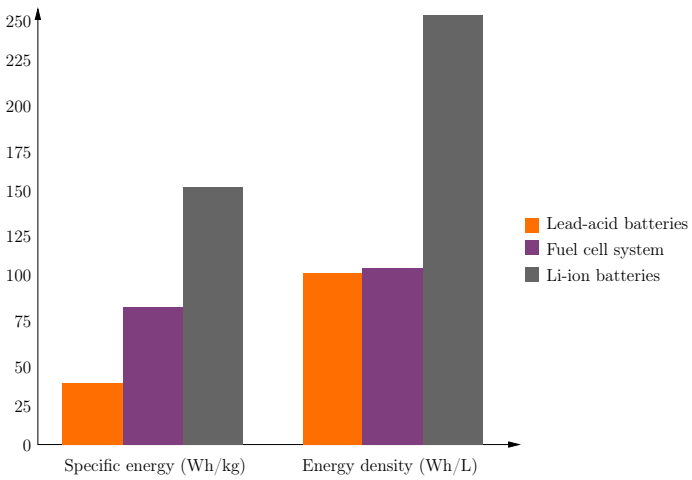

Figure 13. Energy densities comparison between batteries and the investigated fuel cell system

References

[1] M. Michon, J. Duarte, M. Hendrix, and M. Simoes, "A three-port bi-directional converter for hybrid fuel cell systems," in *Power Electronics Specialists Conference, 2004. PESC 04. 2004 IEEE 35th Annual*, vol. 6, 20-25 June 2004, pp. 4736–4742Vol.6.

[2] A. Khaligh, A. Rahimi, Y. Lee, J. Cia, A. Emadi, and S. Andrews, "Digital control of an isolated active hybrid fuel cell/li-ion battery power supply," *IEEE Transactions on Vehicular technology*, vol. 56, no. 6, november 2007.

[3] S. Wang, M. Krishnamurthy, R. Jayabalan, and B. Fahimi, "Quasi-resonant dc/dc converter for high power fuel cells systems," in *Power Electronics Specialists Conference, 2006. PESC '06. 37th IEEE*, 18-22 June 2006, pp. 1–7.

[4] ——, "Low-cost quasi-resonant dc-dc converter for fuel cells with enhanced efficiency," in *Applied Power Electronics Conference and Exposition, 2006. APEC '06. Twenty-First Annual IEEE*, 19-23 March 2006, p. 6pp.

[5] B. Blunier and A. Miraoui, *Piles combustible, Principe, modélisation et applications avec exercices et problèmes corrigés*, ser. Technosup, Ellipses, Ed., 2007, book in French.

[6] ——, "Modelling of fuel cells using multi-domain vhdl-ams language," *Journal of Power Sources*, vol. 177, no. 2, pp. 434–450, 2007.

[7] ——, "Optimization and air supply management of a polymer electrolyte fuel cell," in *IEEE Vehicular Power and Propulsion (VPP), 2005 IEEE Conference*, 7-9 Sept. 2005, p. 7pp.

[8] J. Larminie and J. Lowry, *Electric Vehicle Technology Explained*. John Wiley and Sons, Ltd, 2003.

[9] F. Laurencelle, R. Chahine, J. Hamelin, K. Agbossou, M. Fournier, T. K. Bose, and A. Laperrire, "Characterization of a ballard MK5-E proton exchange membrane fuel cell stack," in *Fuel Cells*, no. 1, 2001, pp. 66–71.